Korean J. Chem. Eng., **22**(4), 528-535 (2005)

The Electrokinetic Microfluidic Flow in Multi-Channels with Emergent Applicability Toward Micro Power Generation

Tae Seok Lee, Myung-Suk Chun†, Dae Ki Choi*, Suk Woo Nam* and Tae-Hoon Lim*

Complex Fluids Research Laboratory, *Environment and Process Technology Div.,
Korea Institute of Science and Technology (KIST), PO Box 131, Cheongryang, Seoul 130-650, Korea
(*Received 17 January 2005 • accepted 9 June 2005*)

Abstract−In order to elaborate the possible applicability of microfluidic power generation from conceptualization to system validation, we adopt a theoretical model of the electrokinetic streaming potential previously developed for the single channel problem. The ion transport in the microchannel is described on the basis of the Nernst-Planck equation, and a monovalent symmetric electrolyte of $LiClO_4$ is considered. Simulation results provide that the flow-induced streaming potential increases with increasing the surface potential of the microchannel wall as well as decreasing the surface conductivity. The streaming potential is also changed with variations of the electric double layer thickness normalized by the channel radius. From the electric circuit model with an array of microchannels, it is of interest to evaluate that a higher surface potential leads to increasing the power density as well as the energy density. Both the power density and the conversion efficiency tend to enhance with increasing either external resistance or number of channels. If a single microchannel is assembled in parallel with the order of 10^3, the power density of the system employing large external resistance is estimated to be above 1 W/m^3 even at low pressure difference less than 1 bar.

Key words: Microfluidics, Electrokinetics, Streaming Potential, Microchannel, Electrolyte Solution, Power Density

INTRODUCTION

Electrokinetic phenomena have been necessarily of concern in the design of diagnostic micro devices and micro-chips [Harrison et al., 1993], particle manipulation techniques [Effenhauser et al., 1997], and micro flow control in micro-electro mechanical system (MEMS) devices [Polson and Hayes, 2000; Yang and Kwok, 2003; Chang and Yang, 2004]. Especially, electrokinetic techniques have the advantage of being easily adaptable into microfluidic systems when compared to external systems [Karniadakis and Beskok, 2003]. Among the electrokinetic phenomena, both electro-osmosis and electrophoresis use an applied electric field to induce motion. On the other hand, both the streaming potential and the sedimentation potential have the opposite electrokinetic coupling in that they use motion to produce an electric field. Basically, such electrokinetic phenomena are present due to the electric double layer (EDL), which forms as a result of the distribution of electric charges near a dielectric charged surface [Hunter, 1981; Probstein, 1994].

Conventional works in the area of electrokinetic transport phenomena mainly focus on electro-osmotic flow. It should also be recognized that the streaming potential has been an emergent technique for surface characterization of materials with solid-liquid interfaces. From the relations involving a quantitative expression of the force that creates the observed electrokinetic phenomena, the measurement of the streaming potential permits the determination of the zeta potential of the hydrodynamic phase boundary [Bowen and Jenner, 1995; Szymczyk et al., 1999; Ren et al., 2001; Sung et al., 2003; Chun et al., 2003]. A relevant work is a new insight recently revealed that the streaming potential is applicable to an electrokinetic micro battery consisting of an array of microchannels [Yang et al., 2003]. Yang et al. conducted analytical solutions on the time-dependent microflow, and found a good agreement between the predicted results and those from experiments with microporous glass filter. Their results suggest the hydrostatic pressure can be converted into electrical work in the order of W/m^3, depending on the properties of the electrolyte solution and channel wall.

Current MEMS and fabrication technologies allow us to predict that the streaming potential technique will become an established process in the field of electrokinetic microfluidics. The streaming potential occurs due to the charge displacement in the EDL caused

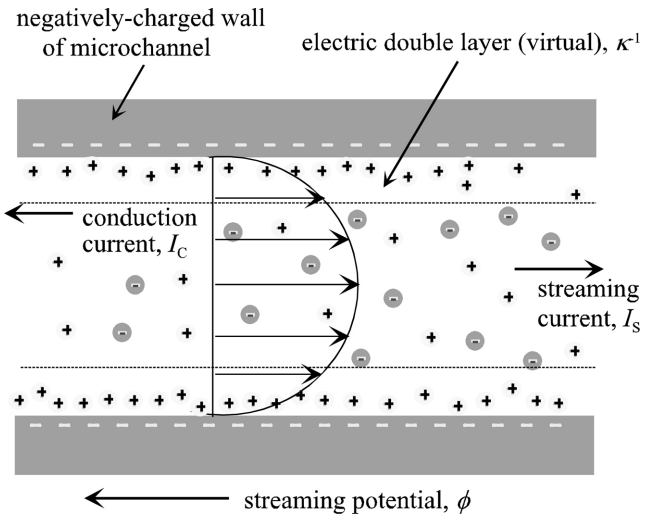

Fig. 1. Schematic view of the development of flow-induced streaming potential along a charged microchannel filled with electrolyte solution.

†To whom correspondence should be addressed.
E-mail: mschun@kist.re.kr

by an external force shifting the liquid phase tangentially against the solid. As illustrated in Fig. 1, the counter-ions in the diffusive (or mobile) part of the EDL are carried toward the downstream end for the applied pressure p. Then the streaming current results in the pressure-driven flow direction of electrolyte solution, and the streaming potential ϕ generates corresponding to this streaming current. This flow-induced streaming potential acts to drive the counter-ions in the mobile part of the EDL to move in the direction opposite to the streaming current. This opposite-directional flow of ions will generate a conduction current in the Stern layer of the EDL. The overall result is a reduced flow rate in the direction of pressure drop referred to as the electroviscous effect [Yang and Li, 1997; Vainshtein and Gutfinger, 2002; Chun, 2002]. The convective transport of hydrodynamically mobile ions can be detected by measuring the streaming potential between the two electrodes positioned at up- and downstream in the liquid flow.

It is the purpose of this paper to evaluate the required performance for applicability toward electrokinetic micro power generation. A theoretical part associated with the single microchannel is that of Chun and co-workers [Chun et al., 2005], who dealt with indepth analysis on microfluidics in a microchannel encompassing electrokinetic phenomena. They developed the momentum equation for an incompressible ionic fluid by verifying the external body force and the relevant flow-induced electric field, from the theoretical analysis of the Navier-Stokes (N-S) equation coupled with the Poisson-Boltzmann (P-B) equation. Basic principle of the net current conservation was faithfully applied in the microchannel taking into account the Nernst-Planck (N-P) equation. In the present study, the flow-induced streaming potential in a multi-channel array is estimated with variations of surface potential, surface conductivity of the microchannel, and bulk electrolyte concentration. As the 1 : 1 type electrolytes, $LiClO_4$ having lower mobility are considered. We estimate the power density as well as the energy density of the electric circuit with variations of design parameters (e.g., pressure difference, the number of channels, and external resistance) in order to address a performance comparison for practical applications. The electric conversion efficiency is also discussed.

ELECTROKINETIC MICROFLOW

We consider a model for pressure-driven and steady-state electrokinetic flow through a uniformly charged straight cylindrical microchannel. Cylindrical coordinates (r, θ, z) are introduced, where r denotes the radial distance from the center axis and z is the distance along the axis of a microchannel. The development of the electrokinetic flow equation extends those of previous works [Rice and Whitehead, 1965; Levine et al., 1975] to symmetric electrolytes in which the mobilities of anions and cations may individually be specified.

For one-dimensional incompressible laminar flow, the velocity of ionic fluid is expressed as $\mathbf{v}=[0, 0, v_z(r)]$, the pressure $p=p(z)$, and the flow-induced electric field $\mathbf{E}=[0, 0, E_z(z)]$. Neglecting gravitational forces, the body force per unit volume ubiquitously caused by the z-directional action of flow-induced electric field E_z on the net charge density ρ_e can be written as $F_z=\rho_e E_z$ [Yang and Li, 1997; Chun, 2002]. The E_z is defined by the flow-induced streaming potential ϕ as $E_z=-d\phi(z)/dz$. With these identities, the N-S equation reduces to

$$\mu\left[\frac{1}{r}\frac{d}{dr}\left(r\frac{dv_z}{dr}\right)\right]=\frac{dp}{dz}-\rho_e E_z \tag{1}$$

where μ is the fluid viscosity. This momentum equation corresponds to the Stokes equation for the flow situation of this study. The boundary conditions applied to $v_z(r)$ are

$$v_z(r)=0 \quad \text{at} \quad r=a, \tag{2a}$$

$$\frac{dv_z(r)}{dr}=0 \quad \text{at} \quad r=0. \tag{2b}$$

Once the charged surface is in contact with an electrolyte, the electrostatic charge would influence the distribution of nearby ions. Then, an electric field is established and the positions of the individual ions in solution are replaced by the mean concentration of ions. It is well-known that the nonlinear P-B equation governing the electric potential field is given as [Hunter, 1981; Probstein, 1994]

$$\nabla^2\Psi=\kappa^2\sinh\Psi \tag{3}$$

Here, the dimensionless electric potential Ψ denotes $Ze\psi/kT$ and the inverse EDL thickness (namely, inverse Debye radial thickness) κ is defined by $\kappa=\sqrt{2n_bZ_i^2e^2/\varepsilon kT}$, where n_b is the electrolyte ionic concentration in the bulk solution at the electroneutral state, Z_i the valence of type i ions, e the elementary charge, ε the dielectric constant, and kT the Boltzmann thermal energy. The n_b ($1/m^3$) equals to the product of the Avogadro's number (1/mol) and bulk electrolyte concentration (mM). The Boltzmann distribution of the ionic concentration of type i (i.e., $n_i=n_b\exp(-Z_ie\psi/kT)$) provides a local charge density Z_ien_i.

The finite difference method evolved in the previous work is applied here and detailed procedure is analogous to the scheme [Chun et al., 2005]. To obtain the solution of the nonlinear P-B equation with the boundary conditions imposed as $\Psi=\Psi_s$ at r=a and $d\Psi/dr=0$ at r=0, the five-point central difference method is taken on the left-hand side of Eq. (3). The $\sinh\Psi$ on the right-hand side can be linearized as $\sinh\Psi_j^k+(\Psi_j^{k+1}-\Psi_j^k)\cosh\Psi_j^k$, where k means the iteration index and the grid index j=1, 2, … N [Chun, 2002]. The finite difference form of the nonlinear P-B equation becomes

$$\frac{\Psi_{j+1}^{k+1}-2\Psi_j^{k+1}+\Psi_{j-1}^{k+1}}{\Delta r^2}+\frac{\Psi_{j+1}^{k+1}-\Psi_{j-1}^{k+1}}{2r_j\Delta r}=\kappa^2[\sinh\Psi_j^k+(\Psi_j^{k+1}-\Psi_j^k)\cosh\Psi_j^k]. \tag{4}$$

Eq. (4) can be solved for Ψ_j^{k+1} by successive iterative calculation, using the value of Ψ obtained in the k-th iteration. From a relation of $\Psi_{-1}^{k+1}=\Psi_1^{k+1}$ encountered in the boundary condition at the center, one can derive as

$$2\Psi_1^{k+1}-[2+(\kappa\Delta r)^2\cosh\Psi_0^k]\Psi_0^{k+1}=(\kappa\Delta r)^2(\sinh\Psi_0^k-\Psi_0^k\cosh\Psi_0^k). \tag{5}$$

From a series of algebraic equations expressed in a matrix form, the electric potential Ψ is obtained and then we can determine the net charge density ρ_e ($\equiv\Sigma_iZ_ien_i=Ze(n_+-n_-)$), as follows

$$\rho_e=Zen_b[\exp(-\Psi)-\exp(\Psi)]=-2Zen_b\sinh\Psi \tag{6}$$

For a high surface potential of $\Psi_s>1$ (i.e., above kT/e=25.69 mV), substituting Eq. (6) into Eq. (1) yields

$$\frac{1}{r}\frac{d}{dr}\left(r\frac{dv_z}{dr}\right)=\frac{1}{\mu}\left(\frac{dp}{dz}\right)-\frac{2Zen_b}{\mu}\sinh\Psi\left(\frac{d\phi}{dz}\right). \quad (7)$$

Eq. (7) takes an integral from 0 to L with respect to z together with setting $\Delta p=p_0-p_L$ and $\Delta\phi=\phi_0-\phi_L$, then we derive a formula for the velocity profile subject to the above boundary conditions as

$$v_z(r)=\frac{a^2-r^2}{4\mu}\left(\frac{\Delta p}{L}\right)-\frac{2Zen_b}{\mu}\left(\frac{\Delta\phi}{L}\right)\int_r^a\frac{1}{r}\left(\int_0^r r\sinh\Psi dr\right)dr \quad (8)$$

where a and L indicate the radius and the length of channel, respectively. Subsequently, one obtains the volumetric flow rate q by $2\pi\int_0^a v_z(r)rdr$.

In the case where the surface of the microchannel wall satisfies a condition of low potential ($\Psi_s\le1$) with a 1 : 1 type electrolyte system, the P-B equation may be linearized corresponding the Debye-Hückel (D-H) approximation [Hunter, 1981; Chun et al., 2003]. For a cylindrical channel, the linearized P-B equation leads to $(1/r)(d/dr)(rd\Psi/dr)=\kappa^2\Psi$, and its solution can be obtained with boundary conditions as $\Psi(r)=\Psi_s I_0(\kappa r)/I_0(\kappa a)$, where I_0 is the modified Bessel function of the first kind of zeroth order. The net charge density is then determined by

$$\rho_e=-\varepsilon\nabla^2\psi=-\varepsilon\kappa^2\psi_s\frac{I_0(\kappa r)}{I_0(\kappa a)}. \quad (9)$$

The analytical solution for velocity profile $v_z(r)$ is derived as

$$v_z(r)=\frac{a^2-r^2}{4\mu}\left(\frac{\Delta p}{L}\right)-\frac{\varepsilon\psi_s}{\mu}\left[1-\frac{I_0(\kappa r)}{I_0(\kappa a)}\right]\left(\frac{\Delta\phi}{L}\right). \quad (10)$$

ELECTROKINETIC FLOW-INDUCED STREAMING POTENTIAL

1. Mathematical Formulation for Single Microchannel

The N-P equation describes the transport of ions in terms of convection and migration resulting from the pressure difference and electric potential gradient, respectively. Diffusion is not considered here due to an assumption of no axial concentration gradient. Ions in the mobile region of the EDL are transported through the single channel, commonly causing the electric convection current (i.e., streaming current) I_S. The accumulation of ions provides the streaming potential difference $\Delta\phi$ (=E_zL). This field causes the conduction current I_C to flow back in the opposite direction. In this case, the net current I consists of I_S and I_C, and it should be zero at the steady state, viz. $I\equiv I_S+I_C=0$ [Werner et al., 1998; Szymczyk et al., 1999; Chun et al., 2003].

The streaming current is defined as an integration of the product of the velocity profile and the net charge density, yielding

$$I_S=2\pi\int_0^a\rho_e(r)v_z(r)rdr. \quad (11)$$

For a low surface potential, Eq. (11) becomes

$$I_S=-\frac{\pi a^2\varepsilon\psi_s}{\mu}\left[1-\frac{2}{\kappa a}\frac{I_1(\kappa a)}{I_0(\kappa a)}\right]\left(\frac{\Delta p}{L}\right)-\frac{\pi a^2\varepsilon^2\kappa^2\psi_s^2}{\mu}\left[1-\frac{2}{\kappa a}\frac{I_1(\kappa a)}{I_0(\kappa a)}-\frac{I_1^2(\kappa a)}{I_0^2(\kappa a)}\right]\left(\frac{\Delta\phi}{L}\right) \quad (12)$$

where I_1 is the modified Bessel function of the first kind of first order. Details for deriving Eq. (12) are provided in Appendix A. The total resistance R along the microchannel consists of the surface resistance R_s and the fluid resistance R_f in parallel [Yang et al., 2003], so that

$$R=\frac{1}{\left(\frac{1}{R_s}+\frac{1}{R_f}\right)}=\frac{R_sR_f}{R_s+R_f}. \quad (13)$$

Using Ohm's rule, the conduction current I_C can then be expressed as

$$I_C\equiv I_{C,s}+I_{C,f}=\frac{\Delta\phi}{R} \quad (14)$$

where $I_{C,s}$ (=$\Delta\phi/R_s$) is the conduction current through the wall and $I_{C,f}$ (=$\Delta\phi/R_f$) is the conduction current through the electrolyte solution. The surface resistance is readily defined as $R_s=L/2\pi a\lambda_s$, where $2\pi a$ equals the wetted perimeter, and λ_s indicates the specific surface conductivity depending on the material property of microchannel.

The fluid resistance certainly varies with the radial position by means of the contribution of radial concentration gradients to the electric current. The influence of an axial concentration gradient upon the conduction current vanishes reasonably. As in the previous study, we invoke again the drift velocity of ion species i, given as [Chun et al., 2005]

$$\mathbf{v}_{d,i}=-Z_ieN_AK_i\nabla\phi \quad (15)$$

where N_A is Avogadro's number and K_i the mobility of ion species i defined as its velocity in the direction of an electric field of unit strength [Bowen and Jenner, 1995; Szymczyk, 1999; Chun et al., 2005]. Now the conduction current through the electrolyte solution for arbitrary channel cross-section can be expressed as follows:

$$I_{C,f}=\int_A\sum_i Z_ien_i\mathbf{v}_{d,i}dA=2\pi Z^2e^2N_A\left(\frac{\Delta\phi}{L}\right)\int_0^a[K_+n_+(r)+K_-n_-(r)]rdr \quad (16)$$

where the subscripts + and − of the ionic number concentration n_i denote the cations and the anions, respectively. Consequently, we obtain the fluid resistance that is addressed as an inverse quantity of the integration of the local fluid conductivity λ_f over the cross-sectional area per channel length:

$$R_f=\frac{L}{2\pi\int_0^a\lambda_f(r)rdr}=\frac{L}{2\pi Z^2e^2N_A\int_0^a[K_+n_+(r)+K_-n_-(r)]rdr}. \quad (17)$$

The total resistance can be identified as

$$R=\frac{L}{2\pi[a\lambda_s+Z^2e^2N_A\int_0^a(K_+n_++K_-n_-)rdr]}. \quad (18)$$

Applying Eqs. (12) and (14) gives an analytic formula of the streaming potential for a low surface potential:

$$\Delta\phi=\frac{\frac{\pi a^2\varepsilon\psi_s}{\mu}\left[1-\frac{2}{\kappa a}\frac{I_1(\kappa a)}{I_0(\kappa a)}\right]\Delta p}{\frac{L}{R}-\frac{\pi a^2\varepsilon^2\kappa^2\psi_s^2}{\mu}\left[1-\frac{2}{\kappa a}\frac{I_1(\kappa a)}{I_0(\kappa a)}-\frac{I_1^2(\kappa a)}{I_0^2(\kappa a)}\right]}. \quad (19)$$

The streaming current for a high surface potential is derived from Eqs. (6), (8), and (11):

$$I_S = -\frac{\pi Z e n_b}{\mu}\left(\frac{\Delta p}{L}\right)\int_0^a r(a^2-r^2)\sinh\Psi dr + \frac{8\pi(Zen_b)^2}{\mu}\left(\frac{\Delta\phi}{L}\right)\int_0^a r\sinh\Psi\left[\int_r^a \frac{1}{r}\left(\int_0^r r\sinh\Psi dr\right)dr\right]dr. \quad (20)$$

We combine the conduction current I_C defined as in Eq. (14), and then finally write the streaming potential as the following expression:

$$\Delta\phi = \frac{\frac{\pi Z e n_b}{\mu}\left[\int_0^a r(a^2-r^2)\sinh\Psi dr\right]\Delta p}{\frac{L}{R} + \frac{8\pi(Zen_b)^2}{\mu}\int_0^a r\sinh\Psi\left[\int_r^a \frac{1}{r}\left(\int_0^r r\sinh\Psi dr\right)dr\right]dr}. \quad (21)$$

In Eq. (21), the electric potential profile is determined by performing the finite difference method, for which the grids of 5×10^3 were built within the channel and the convergence criterion is given as 10^{-8} to satisfy the accuracy requirement.

2. Illustrative Computations

Let us consider a fully developed flow of the aqueous solution in a cylindrical microchannel made of inorganic materials such as either glass or fused silica. The dielectric constant and the viscosity of the fluid are taken as $80\times(8.854\times10^{-12})$ Coul^2/J·m and 1.0×10^{-3} kg/m·sec, at room temperature. The ionic concentration of 1 : 1 type electrolyte equals the solution ionic strength, in which the EDL thickness κ^{-1} (nm) is given by [solution ionic strength (mol)]$^{-1/2}$/3.278. The EDL thicknesses correspond to 3.1, 9.7, and 96.5 for bulk electrolyte concentrations of 10, 1.0, and 10^{-2} mM, where thinning of the EDL means the decrease of electrostatic interaction. The adoption of $LiClO_4$ electrolyte having lower ion mobility was shown to result in a higher streaming potential [Chun et al., 2005]. Its individual mobilities provided in Table 1 can be estimated from a molar conductance of infinite dilution based on the Kohlrausch rule of the migration of ions [Dean, 1999].

Table 1. Each mobility of ions in aqueous solutions at 298.15 K

Monovalent electrolyte	Ions (Cation, Anion)	Mobility (10^{-13} mol·s/kg)
$LiClO_4$	Li^+	4.16
(lithium perchlorate)	ClO_4^-	7.29

Fig. 2 shows the profile of fluid conductivity, i.e., $\lambda_f(r)=Z^2e^2N_A[K_+n_+(r)+K_-n_-(r)]$. The position where the fluid conductivity λ_f reaches the bulk value moves more closely towards the channel wall as κa increases. Here, a κa value of 10 denotes the EDL thickness κ^{-1} is equal to 1 μm. The bulk fluid conductivity has about 1 μS/m at κa= 10, which relatively corresponds to the literature value. A ten times increase in κa results from changes of either a ten times increase in the channel radius for the constant bulk electrolyte concentration or a hundred times increase in the bulk concentration for the constant radius. Fig. 2 allows one to figure out the significance of both the channel radius and the bulk electrolyte concentration as design parameters regarding an efficient tool for electrokinetic micro power generation.

Fig. 3 demonstrates how the streaming potential changes with variations of the surface conductivity λ_s as well as the bulk electrolyte concentration for microchannel radius of 10 μm. Plotting the streaming potential coefficient (=$\Delta\phi/\Delta p$) can verify that simulation results are related to the performance evaluation. The optimum flow rate should be considered to keep up with the pressure drop. The increasing trend in $\Delta\phi/\Delta p$ with decreasing surface conductivity is more considerable for higher surface potential. If Δp of 1 bar is applied the value of streaming potential gains up to about 6 V, although that is a theoretical prediction.

We note that there exists a maximum value of $\Delta\phi/\Delta p$ in Fig. 3. In the low κa region, the rate of an increase in the streaming current is much higher than that of the total resistance R. In fact, the total resistance maintains almost constant compared with the streaming current I_S, appearing as a rise of $\Delta\phi/\Delta p$ with increasing bulk electrolyte concentration. The amount of mobile ions becomes satu-

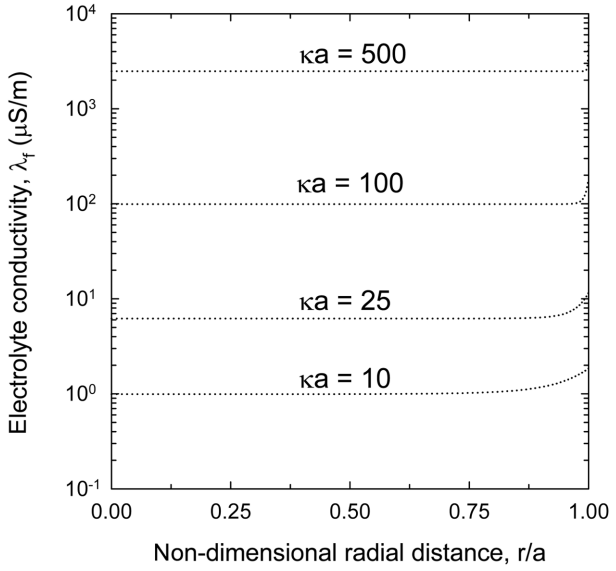

Fig. 2. Fluid conductivity profiles for several dimensionless inverse EDL thicknesses for monovalent electrolyte of $LiClO_4$, where Ψ_s=1 and a=10 μm.

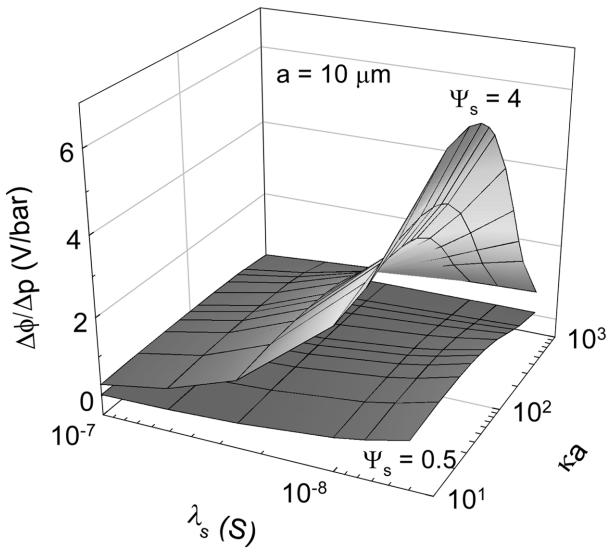

Fig. 3. Effect of bulk concentration of $LiClO_4$ electrolyte on $\Delta\phi/\Delta p$ with different surface conductivities λ_s for Ψ_s=0.5 and 4, where L=10^{-2} m.

rated after a rapid increase in the streaming current; therefore, the streaming current approaches the plateau regime around a maximum point. As the bulk electrolyte concentration continues to increase, the total resistance decreases, whereas the streaming current remains constant. As κa becomes large enough, the streaming potential is almost constant for Ψ_s=0.5. Further, the streaming potential increases with decreasing surface conductivity of the microchannel. Once the surface conductivity becomes lower, a deficiency of the conduction current occurs. Based on the principle of net current conservation, higher streaming potential should necessarily be generated to make up the deficiency.

ELECTRIC CIRCUIT ANALYSIS AND RESULTS

Now, let us hypothesize that the external resistance R_L is applied in the multi-channel array assembled with number of N in parallel, as shown in Fig. 4. Then, the net current equals $N(I_S+I_C)+I_L$, where I_L means the external current. It is taken to be zero at the steady state, viz. $I \equiv N(I_S+I_C)+I_L=0$. In a similar way of deriving Eq. (19) for a low surface potential, the streaming potential in the multi-channel array circuit with external resistance can be obtained:

$$\Delta\phi_L = \frac{\frac{\pi a^2 \varepsilon \psi_s}{\mu}\left[1-\frac{2}{\kappa a}\frac{I_1(\kappa a)}{I_0(\kappa a)}\right]\Delta p}{\frac{L}{R}+\frac{L}{NR_L}-\frac{\pi a^2 \varepsilon^2 \kappa^2 \psi_s^2}{\mu}\left[1-\frac{2}{\kappa a}\frac{I_1(\kappa a)}{I_0(\kappa a)}-\frac{I_1^2(\kappa a)}{I_0^2(\kappa a)}\right]}. \quad (22)$$

The external current passing the external resistance is determined by $I_L=\Delta\phi_L/R_L$. By corresponding analogy for a high potential case,

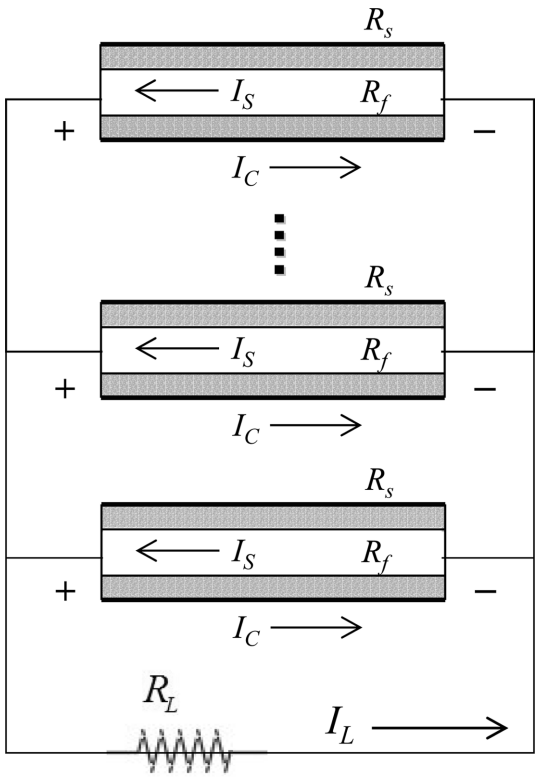

Fig. 4. Schematic diagram of multi-channel array circuit with external resistance.

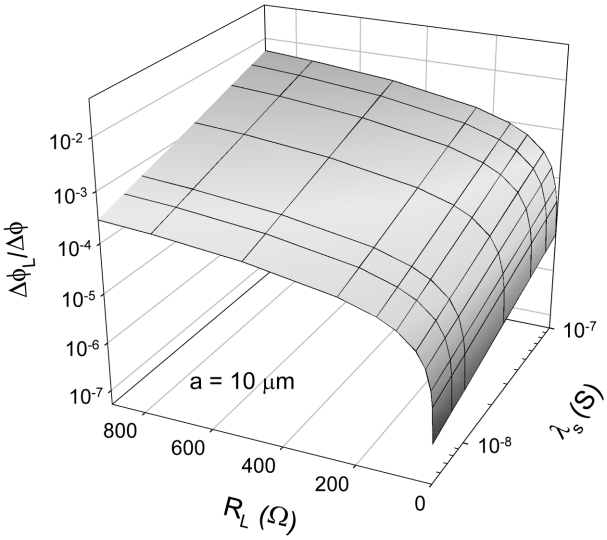

Fig. 5. Effect of external resistance R_L on $\Delta\phi_L/\Delta\phi$ with different surface conductivities λ_s, where Ψ_s=4, κa=50, N=2,000, and L=2×10^{-3} m.

we again derive the streaming potential in this circuit, expressed as

$$\Delta\phi_L = \frac{\frac{\pi Z e n_b}{\mu}\left[\int_0^a r(a^2-r^2)\sinh\Psi dr\right]\Delta p}{\frac{L}{R}+\frac{L}{NR_L}+\frac{8\pi(Zen_b)^2}{\mu}\int_0^a r\sinh\Psi\left[\int_r^a \frac{1}{r}\left(\int_0^r r\sinh\Psi dr\right)dr\right]dr} \quad (23)$$

from which one can determine the external current $I_L=\Delta\phi_L/R_L$. In Fig. 5, an enhancement of the streaming potential $\Delta\phi_L$ in the electric circuit is shown with increasing either the external resistance R_L or the surface conductivity. The enhancement is developed rapidly for smaller R_L, however, a gentle slope is taken with increasing the R_L.

The power density of our system can be evaluated from the electric power divided by the overall volume of microchannels for the imposed external resistance, and the electric power divided by the overall flow rate becomes the energy density, given as, respectively,

$$\text{power density} = \frac{\Delta\phi_L I_L}{N(\pi a^2 L)} = \frac{\Delta\phi_L^2}{N(\pi a^2 L)R_L}, \quad (24a)$$

$$\text{energy density} = \frac{\Delta\phi_L I_L}{Nq} = \frac{\Delta\phi_L^2}{NqR_L}. \quad (24b)$$

We present Fig. 6 for the case of low potential, where higher pressure difference causes the enhancements of both the power density and the energy density as expected. They also increase with increasing either the number of channels or the external resistance. Although the overall trend of Fig. 7 is the same as Fig. 6, the channel wall involving a high surface potential is shown to result in increasing about 70 times the low potential case. Fig. 7 illustrates that, depending on the electrokinetic properties, our theoretical prediction results in the higher order of magnitude for power densities reported in the literature [Koeneman et al., 1997; Yang et al., 2003]. For the number of channels above the order of 10^3, one can observe that the value of power density takes above 1 W/m^3 even at low Δp (i.e., less than 1 bar). Hence, a proper choice of design condition should be considered to obtain the improved performance.

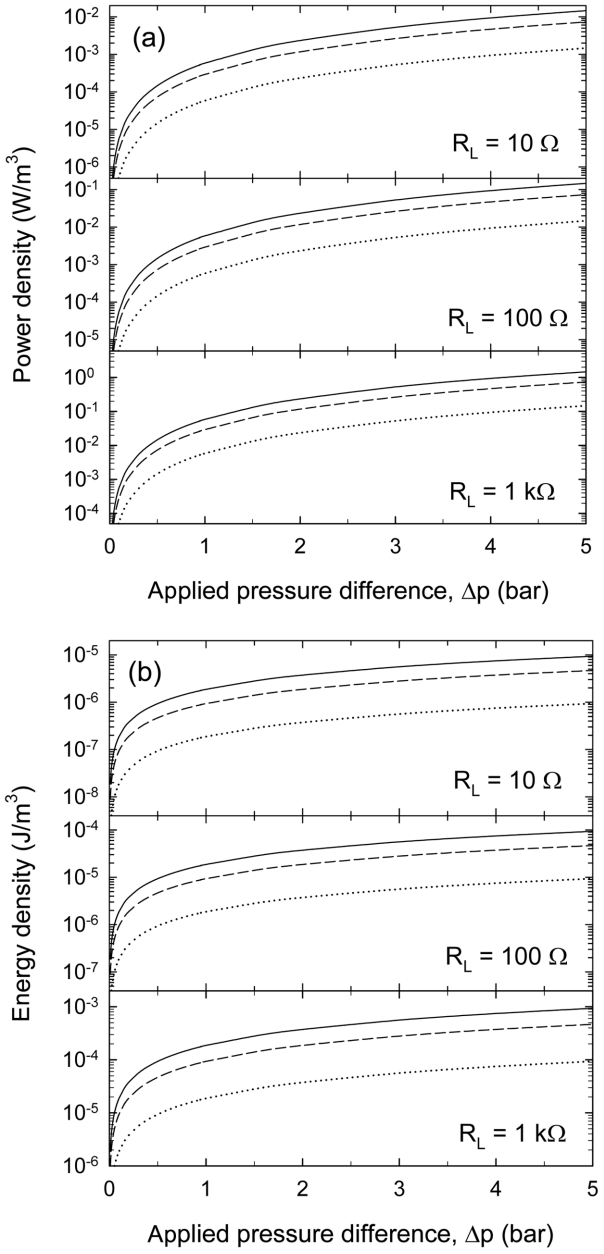

Fig. 6. The predicted power density (a) and energy density (b) as a function of Δp with different external resistances and number of channels for Ψ_s=0.5, a=10 μm, κa=50, L=2×10^{-3} m, and λ_s=5×10^{-9} S; solid curve: N=2,000, dashed curve: N=1,000, dotted curve: N=200.

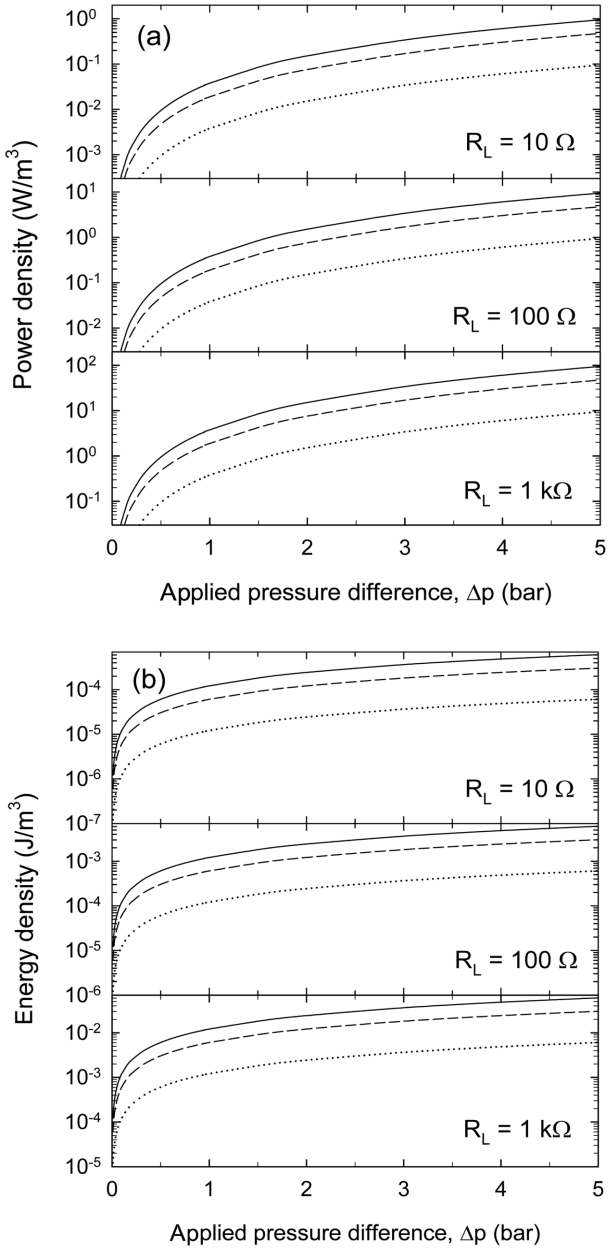

Fig. 7. The predicted power density (a) and energy density (b) as a function of Δp with different external resistances and number of channels for Ψ_s=4, a=10 μm, κa=50, L=2×10^{-3} m, and λ_s=5×10^{-9} S; solid curve: N=2,000, dashed curve: N=1,000, dotted curve: N=200.

We define the electric conversion efficiency as the ratio of the electric work generation to the flow-induced work without the external resistance, as follows:

$$\eta_{eff} = -\frac{\Delta\phi_L I_L}{\Delta\phi N I_S} = -\frac{\Delta\phi_L^2}{\Delta\phi N I_S R_L} \quad (25)$$

Fig. 8 shows the effect of the number of channels N as well as the external resistance R_L upon the conversion efficiency, where the efficiency rises entirely with increasing the N. The efficiency is almost zero for $R_L \rightarrow 0$, because a large I_L can be obtained and the electric work becomes zero. It is evident that the efficiency is increased, as the R_L increases. Further studies remain ahead in order to access the present analysis on a practical system. Instead of the porous glass filter used in the previous work [Yang et al., 2003], we suggest more advantageous MEMS devices such as the microfluidic-chip with multi-channel type.

CONCLUSIONS

This study motivates research on emerging MEMS technologies and relevant micromachining techniques, which have been increasingly employed in the electrokinetic microfluidic system. We em-

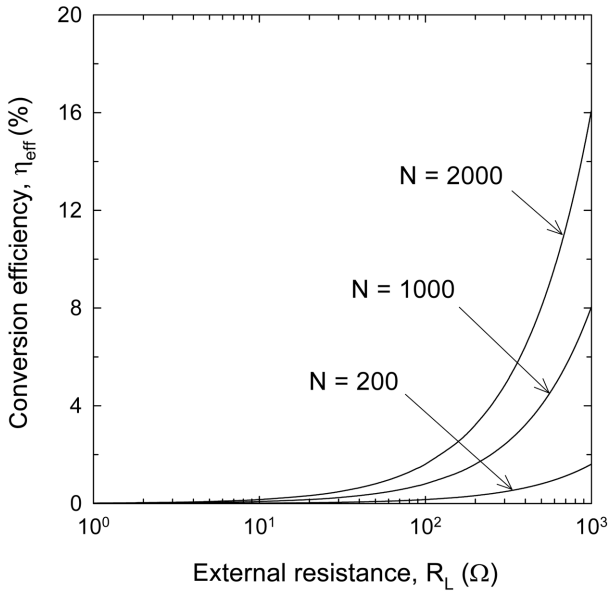

Fig. 8. Effect of external resistance R_L on the conversion efficiency with different number of channels for Ψ_s=4, a=10 μm, κa=50, L=2×10^{-3} m, and λ_s=5×10^{-9} S.

ployed the previously developed analysis concerning the streaming potential due to the electrokinetic microflow in cylindrical microchannels.

A profile of fluid conductivity has been estimated in terms of both the concentration profile and the mobilities of anions and cations. In order to get the design methodology in the system of electrokinetic micro power generation, one should consider the parameter variations of the surface potential of a channel wall, the surface conductivity λ_s, the electrolyte concentration of bulk solution, and the pressure drop across channel Δp. These variations emphasize the system performance.

With increasing surface potential of the wall, the flow-induced streaming potential certainly increases. Both the making up mechanism for the deficiency of conduction current and the principle of net current conservation result in a higher streaming potential with decreasing the surface conductivity. Simulation results show that a maximum value of the streaming potential could be obtained with variations of bulk electrolyte concentration when the microchannel radius is constant. We have shown the feasibility by considering the electric circuit model consisting of an array of circular microchannels. An enhancement of the power density and corresponding energy density as a function of the pressure drop has been observed with increasing either the number of channels or the external resistance.

APPENDIX A: ANALYTICAL SOLUTION FOR LOW POTENTIAL CASE

The relevant equation for streaming current given in Eq. (12) is derived; starting with substitution of Eqs. (9) and (10) into Eq. (11), we write as

$$I_S=-2\pi\int_0^a \varepsilon\kappa^2\psi_s\frac{I_0(\kappa r)}{I_0(\kappa a)}\left\{\left(\frac{a^2-r^2}{4\mu}\right)\left(\frac{\Delta p}{L}\right)-\frac{\varepsilon\psi_s}{\mu}\left[1-\frac{I_0(\kappa r)}{I_0(\kappa a)}\right]\left(\frac{\Delta\phi}{L}\right)\right\}rdr. \quad (A1)$$

It is rearranged as

$$I_S=-\frac{\pi\varepsilon\kappa^2\psi_s}{2\mu}\left(\frac{\Delta p}{L}\right)\int_0^a(a^2-r^2)\frac{I_0(\kappa r)}{I_0(\kappa a)}rdr + \frac{2\pi\varepsilon^2\kappa^2\psi_s^2}{\mu}\left(\frac{\Delta\phi}{L}\right)\int_0^a\frac{I_0(\kappa r)}{I_0(\kappa a)}\left[1-\frac{I_0(\kappa r)}{I_0(\kappa a)}\right]rdr. \quad (A2)$$

The first term in the right-hand side of Eq. (A2) is identified as

$$I_{S,1}\equiv-\frac{\pi\varepsilon\kappa^2\psi_s}{2\mu}\left(\frac{\Delta p}{L}\right)\int_0^a(a^2-r^2)\frac{I_0(\kappa r)}{I_0(\kappa a)}rdr =-\frac{\pi\varepsilon\kappa^2\psi_s}{2\mu I_0(\kappa a)}\left(\frac{\Delta p}{L}\right)\left[a^2\int_0^a rI_0(\kappa r)dr-\int_0^a r^3I_0(\kappa r)dr\right], \quad (A3)$$

and the second one is

$$I_{S,2}\equiv\frac{2\pi\varepsilon^2\kappa^2\psi_s^2}{\mu}\left(\frac{\Delta\phi}{L}\right)\int_0^a\frac{I_0(\kappa r)}{I_0(\kappa a)}\left[1-\frac{I_0(\kappa r)}{I_0(\kappa a)}\right]rdr =\frac{2\pi\varepsilon^2\kappa^2\psi_s^2}{\mu I_0(\kappa a)}\left(\frac{\Delta\phi}{L}\right)\left[\int_0^a rI_0(\kappa r)dr-\frac{1}{I_0(\kappa a)}\int_0^a rI_0^2(\kappa r)dr\right]. \quad (A4)$$

The integral by parts is able to perform using the following:

$$\int_0^a rI_0(\kappa r)dr=\frac{a}{\kappa}I_1(\kappa a) \quad (A5)$$

$$\int_0^a r^3I_0(\kappa r)dr=\frac{a^3}{\kappa}I_1(\kappa a)-\frac{2a^2}{\kappa^2}I_0(\kappa a)+\frac{4a}{\kappa^3}I_1(\kappa a) \quad (A6)$$

$$\int_0^a rI_0^2(\kappa r)dr=\frac{a^2}{2}[I_0^2(\kappa a)-I_1^2(\kappa a)]. \quad (A7)$$

Substituting Eqs. (A5) and (A6) into Eq. (A3) gives

$$I_{S,1}=-\frac{\pi a^2\varepsilon\psi_s}{\mu}\left(\frac{\Delta p}{L}\right)\left[1-\frac{2}{\kappa a}\frac{I_1(\kappa a)}{I_0(\kappa a)}\right], \quad (A8)$$

and substituting Eqs. (A5) and (A7) into Eq. (A4) gives

$$I_{S,2}=-\frac{\pi a^2\varepsilon^2\kappa^2\psi_s^2}{\mu}\left(\frac{\Delta\phi}{L}\right)\left[1-\frac{2}{\kappa a}\frac{I_1(\kappa a)}{I_0(\kappa a)}-\frac{I_1^2(\kappa a)}{I_0^2(\kappa a)}\right]. \quad (A9)$$

Then, the streaming current can be derived as Eq. (12).

ACKNOWLEDGMENT

This work was supported by the Basic Research Fund (Grant No. R01-2004-000-10944-0) from the Korea Science and Engineering Foundations (KOSEF) provided to M.-S.C. We acknowledge financial support as the Future-Oriented Battery Research Fund (2E18270) from the Korea Institute of Science and Technology (KIST).

NOMENCLATURE

A : cross-sectional area of microchannel [m^2]
a : radius of microchannel [m]
E_z : flow-induced electric field in axial direction [V/m]

e : elementary charge [Coul]
F_z : body force in axial direction [N/m^3]
I : net electric current [A]
I_0, I_1 : modified Bessel function of the first kind of zeroth and first order [-]
I_C : conduction current [A]
$I_{C,f}$: conduction current flowing through the bulk electrolyte solution [A]
$I_{C,s}$: conduction current flowing through the microchannel surface [A]
I_L : external current [A]
I_S : streaming current, or convection current [A]
K : mobility of ion species [mol·s/kg]
k : Boltzmann constant [J/K]
L : length of microchannel [m]
N : number of microchannels [-]
n : number concentration of ion species [1/m^3]
p : hydraulic pressure [bar]
q : volumetric flow rate [m^3/s]
R : total resistance of single microchannel [Ω]
R_f : fluid resistance [Ω]
R_L : external resistance [Ω]
R_s : surface resistance [Ω]
r : radial distance in cylindrical coordinates [m]
t : time [s]
T : absolute temperature [K]
v : fluid velocity component [m/s]
$\mathbf{v}_d$: drift velocity of ion species [m/s]
Z : valence of ion species [-]
z : axial distance in cylindrical coordinates [m]

Greek Letters

ε : dielectric constant, or permittivity of the medium [Coul^2/J·m]
η_{eff} : conversion efficiency [-]
κ : inverse EDL thickness [1/m]
λ_f : fluid conductivity [S/m]
λ_s : specific surface conductivity [S]
μ : fluid viscosity [kg/m·s]
ρ_e : net charge density [Coul/m^3]
ϕ : flow-induced streaming potential [V]
ϕ_L : streaming potential in the circuit with external resistance [V]
Ψ : dimensionless electric potential [-]
Ψ_s : dimensionless electric surface potential [-]
ψ : electric potential [V]
ψ_s : electric surface potential [V]

REFERENCES

Bowen, W. R. and Jenner, F., "Electroviscous Effects in Charged Capillaries," *J. Colloid Interface Sci.*, **173**, 388 (1995).

Chang, C. C. and Yang, R. J., "Computational Analysis of Electrokinetically Driven Flow Mixing in Microchannels with Patterned Blocks," *J. Micromech. Microeng.*, **14**, 550 (2004).

Chun, M.-S., "Electrokinetic Flow Velocity in Charged Slit-like Microfluidic Channels with Linearized Poisson-Boltzmann Field," *Korean J. Chem. Eng.*, **19**, 729 (2002).

Chun, M.-S., Lee, S.-Y. and Yang, S.-M., "Estimation of Zeta Potential by Electrokinetic Analysis of Ionic Fluid Flows through a Divergent Microchannel," *J. Colloid Interface Sci.*, **266**, 120 (2003).

Chun, M.-S., Lee, T. S. and Choi, N. W., "Microfluidic Analysis on Electrokinetic Streaming Potential Induced by Microflows of Monovalent Electrolyte Solution," *J. Micromech. Microeng.*, **15**, 710 (2005).

Dean, J. A. (eds.), *Lange's Handbook of Chemistry*, 15th Ed., McGraw-Hill, New York (1999).

Effenhauser, C. S., Bruin, G. J., Paulus, A. and Ehrat, M., "Integrated Capillary Electrophoresis on Flexible Silicone Microdevices: Analysis of DNA Restriction Fragments and Detection of Single DNA Molecules on Microchips," *Anal. Chem.*, **69**, 3451 (1997).

Harrison, J. D., Fluri, K., Seiler, K., Fan, Z. H., Effenhauser, C. S. and Manz, A., "Micromachining a Miniaturized Capillary Electrophoresis-based Chemical Analysis System on a Chip," *Science*, **261**, 895 (1993).

Hunter, R., *Zeta Potential in Colloid Science: Principles and Applications*, Academic Press Inc., London (1981).

Karniadakis, G. E. and Beskok, A., *Micro Flows: Fundamentals and Simulation*, Springer-Verlag Inc., New York (2003).

Koeneman, P. B., Busch-Vishniac, I. J. and Wood, K. L., "Feasibility of Micro Power Supplies for MEMS," *J. Microelectromech. Syst.*, **6**, 355 (1997).

Levine, S., Marriott, J. R., Neale, G. and Epstein, N., "Theory of Electrokinetic Flow in Fine Cylindrical Capillaries at High Zeta-potentials," *J. Colloid Interface Sci.*, **52**, 136 (1975).

Polson, N. A. and Hayes, M. A., "Electroosmotic Flow Control of Fluids on a Capillary Electrophoresis Microdevice using an Applied External Voltage," *Anal. Chem.*, **72**, 1088 (2000).

Probstein, R. F., *Physicochemical Hydrodynamics*, Wiley and Sons, New York (1994).

Ren, L., Li, D. and Qu, W., "Electro-Viscous Effects on Liquid Flow in Microchannels," *J. Colloid Interface Sci.*, **233**, 12 (2001).

Rice, C. L. and Whitehead, R., "Electrokinetic Flow in a Narrow Cylindrical Capillary," *J. Phys. Chem.*, **69**, 4017 (1965).

Sung, J. H., Chun, M.-S. and Choi, H. J., "On the Behavior of Electrokinetic Streaming Potential During Protein Filtration with Fully and Partially Retentive Nanopores," *J. Colloid Interface Sci.*, **264**, 195 (2003).

Szymczyk, A., Aoubiza, B., Fievet, P. and Pagetti, J., "Electrokinetic Phenomena in Homogeneous Cylindrical Pores," *J. Colloid Interface Sci.*, **216**, 285 (1999).

Vainshtein, P. and Gutfinger, C., "On Electroviscous Effects in Microchannels," *J. Micromech. Microeng.*, **12**, 252 (2002).

Werner, C., Körber, H., Zimmermann, R., Dukhin, S. and Jacobasch, H.-J., "Extended Electrokinetic Characterization of Flat Solid Surfaces," *J. Colloid Interface Sci.*, **208**, 329 (1998).

Yang, C. and Li, D., "Electrokinetic Effects on Pressure-Driven Liquid Flows in Rectangular Microchannels," *J. Colloid Interface Sci.*, **194**, 95 (1997).

Yang, J. and Kwok, D. Y., "Analytical Treatment of Flow in Infinitely Extended Circular Microchannels and the Effect of Slippage to Increase Flow Efficiency," *J. Micromech. Microeng.*, **13**, 115 (2003).

Yang, J., Lu, F., Kostiuk, L. W. and Kwok, D. Y., "Electrokinetic Microchannel Battery by Means of Electrokinetic and Microfluidic Phenomena," *J. Micromech. Microeng.*, **13**, 963 (2003).